



New mesoporous silicotitaniumphosphate and its application in acid catalysis and adsorption of As(III/V), Cd(II) and Hg(II)

Manidipa Paul^a, Nabanita Pal^a, M. Ali^b, Asim Bhaumik^{a,*}

^a Department of Materials Science, Indian Association for the Cultivation of Science, 2A & B Raja S. C. Mullick Road, Jadavpur, Kolkata, West Bengal 700 032, India

^b Chemistry Department, Jadavpur University, Jadavpur, Kolkata, West Bengal 700 032, India

ARTICLE INFO

Article history:

Received 24 December 2009
Received in revised form 2 April 2010
Accepted 1 July 2010
Available online 7 July 2010

Keywords:

Adsorption
Benzylation reaction
Heteroelement incorporation
Mesoporous materials
Titanium phosphate

ABSTRACT

A new mesoporous silicotitaniumphosphate material has been synthesized by using a non-conventional phosphorous source trimethyl phosphite with the aid of Pluronic F127 as structure directing agent (SDA). The mesopores are generated due to the slow hydrolysis of the reactant materials in the presence of supramolecular-assembly of non-ionic surfactant under the evaporation induced self-assembly (EISA) process. The material has been characterized by powder XRD, N₂ sorption, TEM, SEM-EDS, TG-DTA, FT-IR, XPS, ²⁹Si, ³¹P MAS NMR and UV-vis spectroscopic techniques. This new mesoporous material has considerably high BET surface area (379 m² g⁻¹) and narrow pore size distribution with a peak pore width of 5.4 nm. The material showed good catalytic activity in the liquid phase Friedel-Crafts benzylation reaction suggesting strong acidity on its surface. It can also be used as good adsorbent for the removal of toxic metal ions As(III/V), Cd(II) and Hg(II) from the contaminated water.

© 2010 Elsevier B.V. All rights reserved.

1. Introduction

Since the discovery of mesoporous silica molecular sieves using the supramolecular-assembly of surfactants as SDA [1,2], the door for a new area of research is opened to the researchers. The very high surface area, tunable pore size, easy functionalization and large diversity of frameworks have made this class of material an efficient catalyst, adsorbent and an excellent host for the nanomaterial synthesis. In the last few years attentions have also been focused to explore different types of mesoporous materials other than silica framework like metal oxides, phosphates, carbon, etc. Functionalized mesoporous materials have received much interest in this context due to their wide application in various catalytic reactions [3–5]. Recently several porous metallophosphates [6–9] have been reported, which could find important applications as catalyst in selective organic reactions [8], exchanger [9] and photocatalysis [10]. Mesoporous materials containing different hetero-elements find various practical applications due to the specific physical and chemical nature of the doped element in the framework. Although the mesoporous titanium phosphates synthesized using cationic and anionic surfactants as SDA have been exploited as catalysts for liquid phase oxidation and photocatalytic reactions, their potentiality in acid catalyzed reactions have not been studied so far. Moreover the

stability of these phosphate-based mesoporous materials is relatively poor due to the highly charged framework structure. On the other hand, multi-component mesoporous phosphate-based materials [11] have better stability and high surface area. But to date, their catalytic properties in liquid phase reactions have not been explored so far.

This problem can be overcome by introducing Si in the mesoporous titanium phosphate framework similar to the incorporation of Si in the aluminophosphate [12,13] or tin(IV) phosphate materials [14]. Herein, we report the synthesis of novel mesoporous silicotitaniumphosphate material having very high surface area and thermal stability. The material also exhibits a good catalytic activity in benzylation reaction. To the best of our knowledge there is no report of mesoporous silicotitaniumphosphate material in the literature. Furthermore in this synthetic procedure we have chosen Pluronic F127 as template, which generally plays a crucial role for the formation of silica [15] and metal oxide [16] mesophases using evaporation induced self-assembly (EISA) method. The main advantage of this procedure is that here we can adjust the molar ratio of the constituents in the precursor gel, as the ratio remain almost same in gel and final calcined product. This novel material showed good adsorption property and catalytic activity in liquid phase benzylation reaction.

2. Experimental

Mesoporous silicotitaniumphosphate has been synthesized using titanium (IV) butoxide (Ti(BuO)₄, Aldrich) as the source of

* Corresponding author. Fax: +91 33 2473 2805.

E-mail addresses: msab@iacs.res.in, msab@mahendra.iacs.res.in (A. Bhaumik).

Table 1
Physico-chemical properties of mesoporous silicotitaniumphosphate sample.

Sample	Surface Si:Ti:P mole ratio		BET surface area ($\text{m}^2 \text{g}^{-1}$)	Adsorption capacity (mmol g^{-1})
	Gel	Solid		
MSTP-Cal	1:1:0.5	0.87:0.8:0.5	379	0.8

titanium. Trimethyl phosphite (TMP, Spectrochem) and tetraethylorthosilicate (TEOS, Aldrich) were used here as phosphorous and silica precursors, respectively. Triblock co-polymer Pluronic F127 (Aldrich) was used as structure directing agent (SDA) in the presence of concentrated hydrochloric acid (HCl, Merck, 35% aqueous) and acetic acid (AcOH, Merck, 100% glacial). In a typical synthetic procedure, first 2.4 g Pluronic F127 was dissolved in 30 ml of absolute ethanol with the addition of 2.4 g of acetic acid and 2.5 g of conc. HCl under vigorous stirring. The mixture was covered with a PE film and stirred at room temperature until it dissolved completely. Then 3.4 g of titanium (IV) butoxide was added to the above mixture and the mixture was stirred for another 1 h before 2.08 g of TEOS was added. TEOS was then allowed to hydrolyze in the acidic medium followed by the addition of 0.62 g of TMP to the synthetic gel. After gelation at 313 K (relative humidity was controlled at ~40%) for 1 day, the gel was transferred in an oven at 333 K and aged for 3 days. The molar ratio of the various constituents in the gel was 0.19 F127: 514.0 EtOH: 10.0 $\text{Ti}(\text{BuO})_4$: 5.0 TMP: 40.0 AcOH: 24.0 HCl: 10.0 TEOS. The resulting pale-yellow colored solid powder material was calcined in the flow of air at 673 K for 6 h to remove the template. The as-synthesized and calcined samples have been designated as MSTP-As and MSTP-Cal, respectively.

Powder X-ray diffraction patterns of the materials were recorded on a Bruker D-8 Advance diffractometer operated at 40 kV voltage and 40 mA current and calibrated with a standard silicon sample, using Ni-filtered $\text{Cu K}\alpha$ ($\lambda = 0.15406 \text{ nm}$) radiation. Nitrogen adsorption/desorption isotherms were obtained using a Beckman Coulter SA 3100 surface area analyzer at 77 K. Before the measurement, the sample was degassed at 423 K for 3 h. TEM images were recorded in a Jeol JEM 2010 transmission electron microscope. JEOL JEM 6700F field emission scanning electron microscope with an energy dispersive X-ray spectroscopic (EDS) attachment was used to record the morphology of the sample and its surface chemical composition. FT-IR spectra of these samples were recorded on KBr pellets by using a Nicolet MAGNA-FT IR 750 spectrometer series II. UV-visible diffuse reflectance spectra were obtained by using a Shimadzu UV 2401PC spectrophotometer with an integrating sphere attachment and BaSO_4 pellet was used as background standard. Thermogravimetry (TG) study and differential thermal analysis (DTA) were carried out in a thermal analyzer TA SDT Q-600. ^{29}Si and ^{31}P solid state magic angle spinning nuclear magnetic resonance (MAS NMR) experiments were carried out to evaluate the different chemical environment of the Si and P atoms in the mesoporous matrix. Bruker advance 500 spectrometer was used here for NMR data recording. Tetramethylsilane (TMS) and phosphoric acid were used as reference for chemical shift measurement for ^{29}Si and ^{31}P , respectively. X-ray photoelectron spectrum (XPS) of the mesoporous silicotitaniumphosphate sample was recorded in VG Microtech Clam 2 Analyzer using Mg K-alpha X-ray source. The spectrum was calibrated taking the reference of C 1s peak at 284.5 eV.

The liquid phase benzylation reactions were carried out in a 50 ml two necked round bottom flask equipped with a reflux condenser and septum. The reactions were carried out at 348 K by using a temperature controlled oil-bath. The substrate and the benzylation agent i.e. benzyl chloride was added to the catalyst in a required molar ratio (10:1). The catalyst was pretreated at 673 K for 4 h prior to the reaction. Aliquots were withdrawn at a regular interval from the reaction mixture and analyzed using a gas chromatograph (Agilent

7890 A) equipped with a FID detector and fitted with a capillary column. The conversion was calculated based on the amount of the benzylation agent.

For measuring the ion-exchange efficiency of the MSTP-Cal, 0.05 g of the sample was taken in 40 ml 0.01 M KCl solution and the mixture was stirred for 2 h. Then the solution was filtered. The Cl^- concentration in the initial KCl solution and in the final filtrate solutions were determined through titration by using a 0.01 M AgNO_3 solution. In the titration 5% potassium chromate aqueous solution was used as indicator. Then the exchanged Cl^- concentration and hence the anion exchange capacity was measured by subtracting the Cl^- ion concentration in the filtrate from the initial one.

3. Results and discussion

3.1. Synthetic strategy and chemical composition

Here the synthesis of mesoporous silicotitaniumphosphate has been carried out by the slow evaporation method. For the preparation of the synthesis gel very highly acidic medium has been employed as only at this low pH the template F127 can form micelle through H-bonding interactions [15,16]. Acetic acid here plays the role of a complexing agent to stabilize Ti(IV). The key factor of this synthesis is slow hydrolysis of the constituents. For this reason $\text{Ti}(\text{t-BuO})_4$ and TMP is used here instead of other common titanium and phosphorous sources. The gel preparation is carried out in absence of water and absolute alcohol is used as solvent. Surface chemical composition of the mesoporous silicotitaniumphosphate material is given in Table 1. As seen from the table that Si/Ti mole ratio in MSTP-Cal is 1.08, which is very similar to the synthesis gel mixture.

3.2. Powder XRD

The small angle powder XRD pattern of MSTP-Cal sample is shown in Fig. 1. A single peak for d_{100} plane is observed at 2θ value 1.05, which indicates that sample has mesopores in the framework

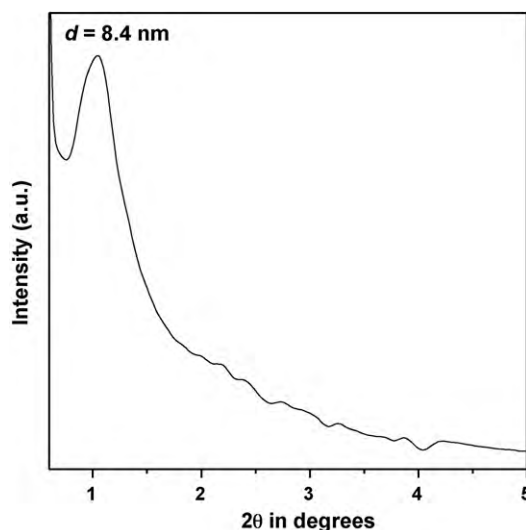


Fig. 1. Powder XRD pattern of the MSTP-Cal.

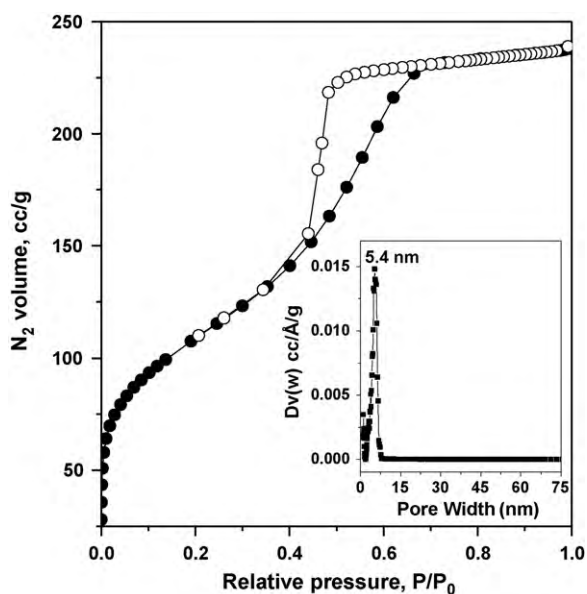


Fig. 2. N_2 adsorption (●)/desorption (○) isotherms and pore size distribution (inset) of the MSTP-Cal.

structure but devoid of any long range mesoscopic ordering. The 2θ value corresponds to an average inter-pore separation of 8.1 nm. The wide angle XRD pattern (not shown) clearly indicates amorphous nature of the sample and absence of any impurity TiO_2 and/or condensed phosphate phases.

3.3. Surface area and pore size distribution

In Fig. 2 N_2 adsorption–desorption isotherms of MSTP-Cal sample are shown. As seen from the figure that the isotherms are of type IV in nature, having capillary rise at higher P/P_0 together with hysteresis loop, indicating the existence of large cylindrical mesopores [17,18]. Brunauer–Emmett–Teller (BET) surface area of the sample calculated from this isotherm is $379 \text{ m}^2 \text{ g}^{-1}$. Pore size distribution (PSD) of the sample estimated from these isotherms by using non-local density functional theory (NLDFT, inset of Fig. 2) suggested the average pore width is ca. 5.4 nm.

3.4. Morphology study

The transmission electron microscopy (TEM) image of this calcined MSTP-Cal sample is shown in Fig. 3. The presence of low electron density spherical spots of 5.0–6.0 nm diameters, corresponding to the large size mesopores and their disordered wormhole-like arrangements. Thus from TEM images and the small angle XRD data we can conclude that this mesoporous silicotitaniumphosphate material has disordered wormhole structure. The average mesopore dimension obtained from the PSD pattern of the N_2 sorption isotherms is also nearly same with that obtained from the TEM image analysis. Textural property and particle size of the mesoporous material were investigated from the scanning electron microscopy (SEM). Typical morphology of the sample is displayed in Fig. 4, showing large aggregates formed with very tiny spherical nanoparticles having dimensions of 15–20 nm. Chemical analysis data (using EDS) is shown in the bottom of Fig. 4, confirming that Ti, Si, P and O distributed uniformly in MSTP-Cal sample.

3.5. Metal–template interaction

The nature of framework and bonding of the as-synthesized and calcined mesoporous silicotitaniumphosphate samples (Fig. 5)

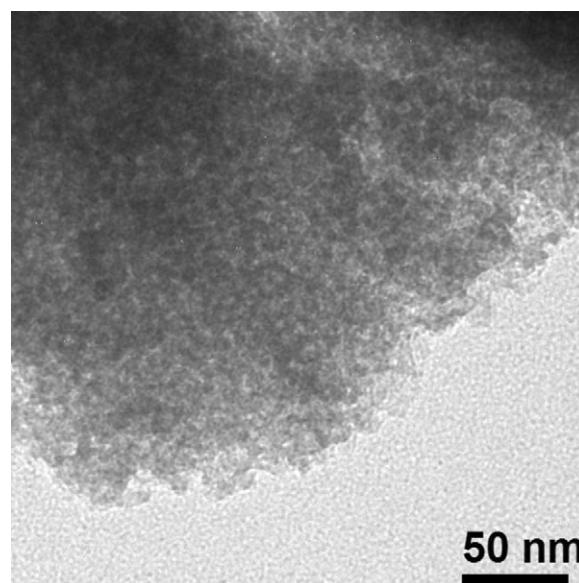


Fig. 3. TEM image of the MSTP-Cal.

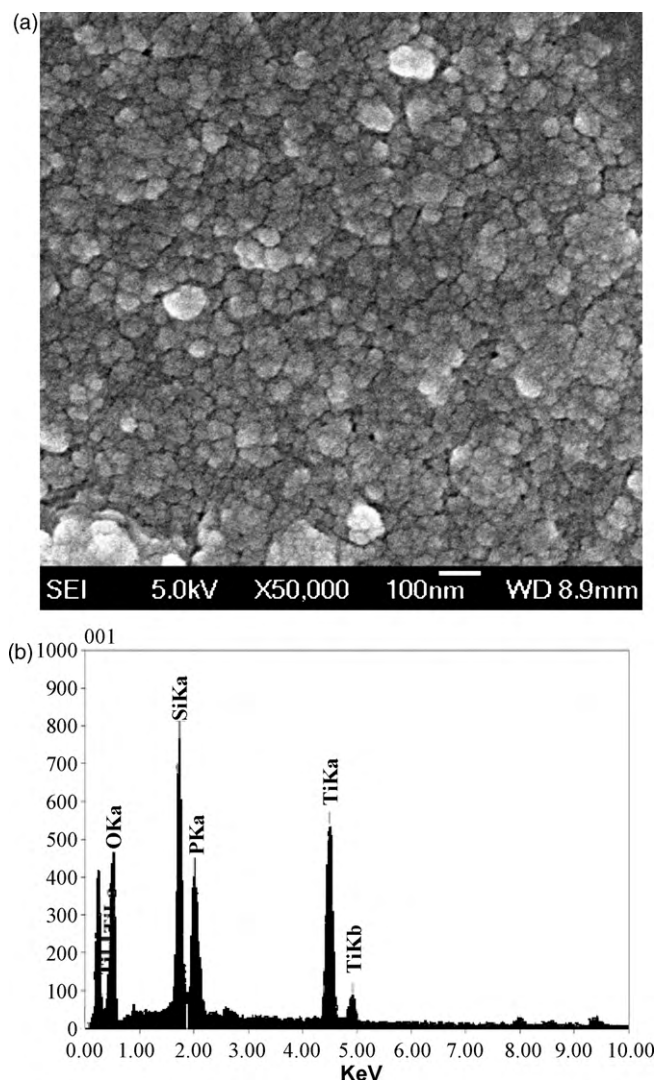


Fig. 4. SEM image of the MSTP-Cal (a) and its EDS pattern (b).

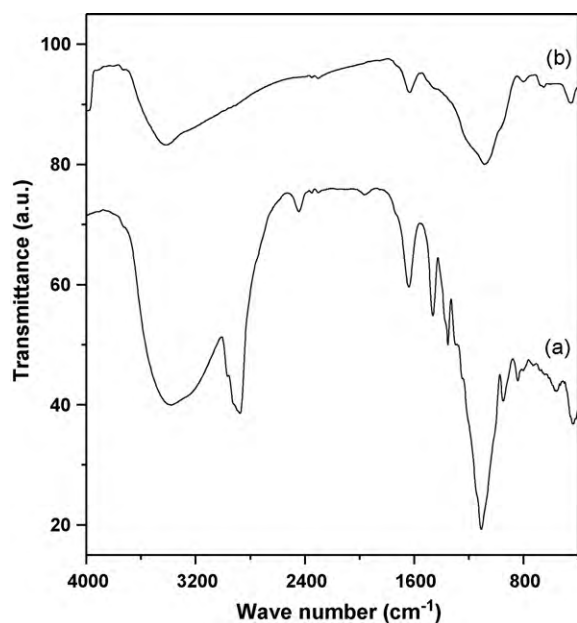


Fig. 5. FT-IR spectra of the as-synthesized MSTP-As (a) and calcined MSTP-Cal (b).

are obtained from FT-IR spectral analysis. According to the literature [19] the broad band coming near 3400 cm^{-1} attributed to O–H stretching vibration and a low intense peak near 1630 cm^{-1} is the deformation vibration for H–O–H bonds of the physically adsorbed moisture. The peak coming at $2850\text{--}3000$ and 1115 cm^{-1} for the as-synthesized sample are assigned to the C–H and C–O–C stretching vibration of F127, which is absent in the calcined sample due to the removal of surfactant after high temperature heat treatment. The wide band near $1050\text{--}1130\text{ cm}^{-1}$ could be attributed to Ti–O–P framework vibration [20] and the band obtained at 1230 cm^{-1} due to P–O–H bond. Another band obtained at 665 cm^{-1} indicates the presence of O–P–O stretching, whereas vibration at 568 cm^{-1} [21] indicates the presence of Ti–O bond. The peak at 946 cm^{-1} could be attributed to the Si–O–H stretching. Absence of peak at 1090 cm^{-1} suggests that no Si–O–Si bond is present in the framework structure [22] of silicotitanium phosphate.

3.6. Optical study

Fig. 6 represents the UV–visible spectra of MSTP-Cal along with bulk titania. Compared to bulk titania, MSTP-Cal shows a blue shift in absorption band (331 and 300 nm , respectively). The absorption band coming in the wavelength region 300 nm is mainly due to the electronic transition from $O^{2-} 2p$ to $Ti^{4+} 3d$ orbital. A similar high-energy absorption edge due to tetrahedral co-ordination of Ti has been observed for mesoporous titanasilicate [23], Ti-exchanged Y-zeolites [24] and heteroelement doped TiO_2 nanostructured materials [25]. The high-energy absorption band indicates that the tetrahedral co-ordination of Ti is dominant in mesoporous silicotitaniumphosphate sample.

3.7. Thermal analysis

In Fig. 7, the thermogravimetric (TG) and differential thermal analysis (DTA) data are shown for the as-synthesized mesoporous silicotitaniumphosphate sample. From the figure it is seen that ca. 10 wt.% loss has taken place up to 495 K in the TGA curve, which is actually composed of two steps. The first step is accompanied with a sharp wt. loss of ca. 7.3% followed by a gradual decrease at elevated temperature. This is because of the removal of the adsorbed water molecule from the surfaces. No such distinct peak is observed in

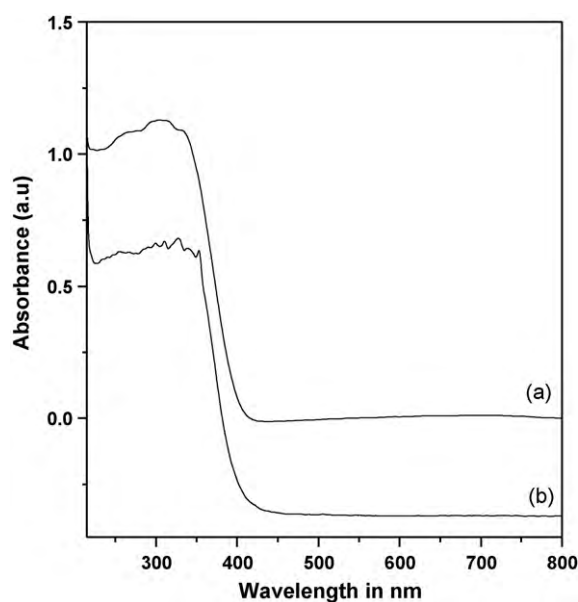


Fig. 6. UV–visible diffuse reflectance spectra of the MSTP-Cal (a) and TiO_2 (b).

the DTA curve at the temperature range $302\text{--}496\text{ K}$ which suggests that the sample is stable up to 496 K . A sharp wt loss of ca. 44.2% is occurred at the temperature range $496\text{--}650\text{ K}$, which is mainly due to the removal of the organic SDA molecules from the MSTP-As. In the DTA curve also we observed a sharp exotherm at 641 K , indicating the decomposition of F127 molecules.

3.8. XPS study

Fig. 8a shows the high-resolution XPS spectra of Ti 2p electron on our calcined mesoporous silicotitaniumphosphate material. The XPS spectra of the Ti 2p region are composed of two peaks. The binding energies for Ti $2p_{3/2}$ and Ti $2p_{1/2}$ are 459.2 and 465.4 eV . Titanium (IV) atoms located at the tetrahedral positions in the titanium silicate framework of TS-1 have Ti $2p_{3/2}$ and Ti $2p_{1/2}$ binding energies of 460 and 466 eV , respectively [26,27] whereas for octahedral co-ordination these energies correspond to 458 and 464 eV , respectively. As in our sample the peaks come at 459.2 and 465.4 eV so it confirms that a majority of the titanium species

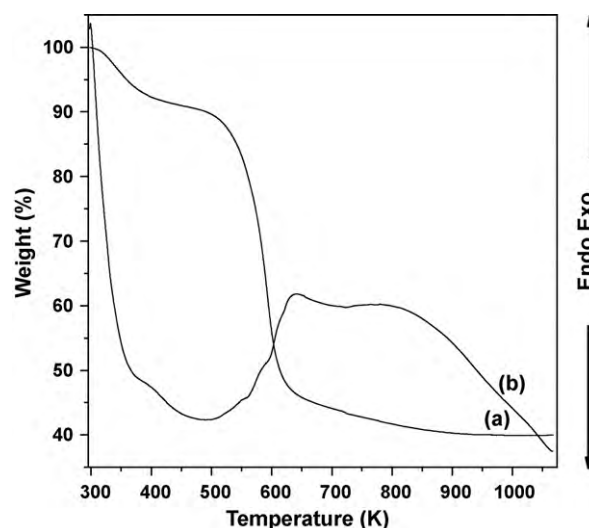


Fig. 7. TG (a) and DTA (b) curves for the as-synthesized MSTP-As sample.

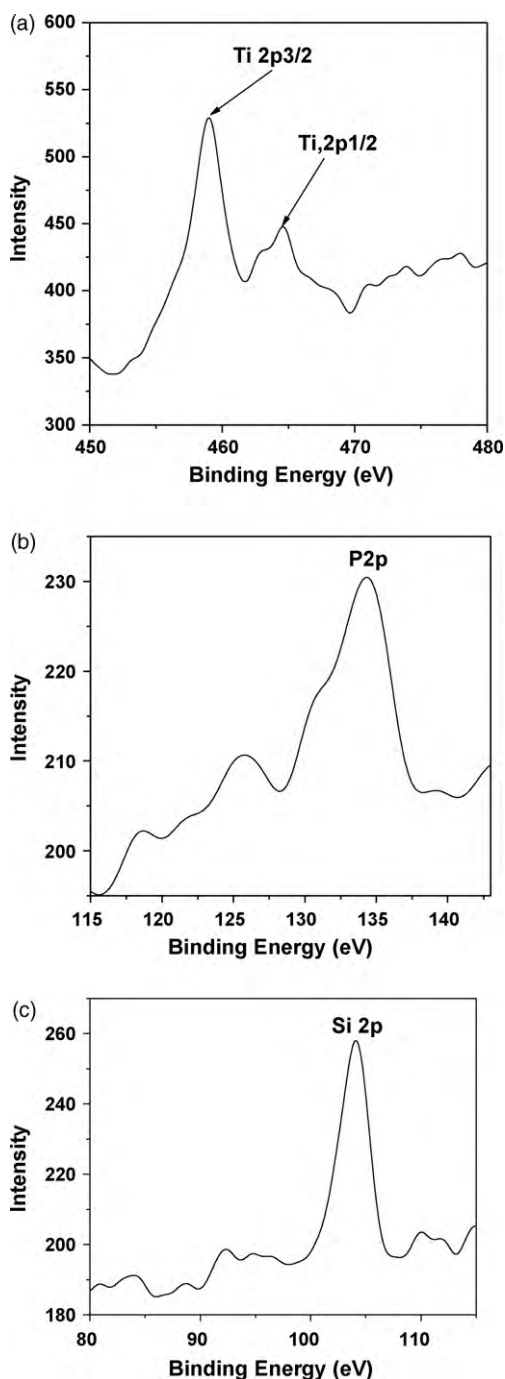


Fig. 8. PS of Ti 2p (a), P 2p (b) and Si 2p (c) of MSTP-Cal.

in our sample is Ti(IV) and they are tetrahedrally co-ordinated. P 2p binding energy for MSTP-Cal (Fig. 8b) is observed at 134.4 eV, indicating the pentavalent state of P in the material. Absence of any peak near 128.6 eV, which is usually attributed to the binding energy of Ti–P bond [28,29] suggested that there is no bonding between Ti and P present in our MSTP-Cal material. In Fig. 8c XPS spectrum of Si 2p is shown. As seen from the spectrum that signal observed at 104.23 eV [30], confirms the presence of tetrahedral Si in the framework of mesoporous silicotitaniumphosphate.

3.9. ^{29}Si and ^{31}P solid state MAS NMR study

^{29}Si chemical shifts of silicates are often utilized as an important tool to understand the local environment of the T-atoms connected

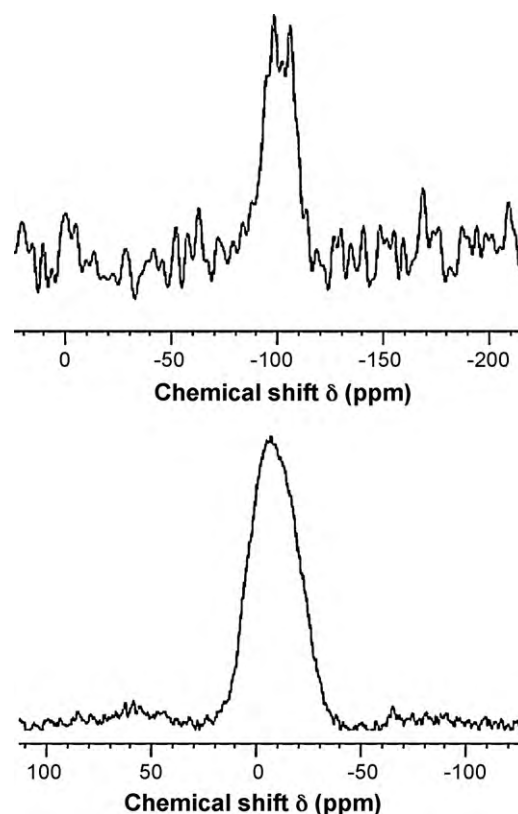


Fig. 9. ^{29}Si (up) and ^{31}P (down) MAS NMR of MSTP-Cal.

with a SiO_4 tetrahedral unit [31]. ^{29}Si MAS NMR spectrum of MSTP-Cal is shown in Fig. 9 (up). From the figure it is clear that there are two major Si species corresponding to chemical shifts at ca. -105.2 and -95.6 ppm. These could be attributed to the Ti(IV) substitution in $\text{Si}(\text{OSi})_4$ (Q_4) and $\text{Si}(\text{OH})(\text{OSi})_3$ (Q_3) environments, respectively [31]. Considerable downfield chemical shifts for all these peak maxima vis-à-vis pure mesoporous silica SBA-15 [32] suggested P and Ti incorporation adjacent to the SiO_4 tetrahedral units. The presence of Ti and P atoms in the vicinity of SiO_4 tetrahedra may also create $\text{Si}(3\text{Si}, \text{Ti}/\text{P})$ and $\text{Si}(2\text{Si}, 2\text{Ti}/\text{P})$ like local environments, which could contribute significantly to the large downfield chemical shifts. On the other hand the ^{31}P MAS NMR spectra of the titanium phosphate samples showed a broad signal with chemical shifts between 10 and -25 ppm (Fig. 9, down). This peak can be assigned to a mixture of tetrahedral P environments with connectivity 3 and 4 [$\text{P}(\text{OTi})_3\text{OH}$ and $\text{P}(\text{OTi})_4$]. Tetrahedral phosphorus in mesoporous titanium phosphate materials shows a strong sharp band at ca. -5.4 to -9.8 ppm [9]. Thus these ^{29}Si and ^{31}P MAS NMR experiments revealed the presence of tetrahedral Si and P species inside the network of mesoporous silicotitaniumphosphate material.

3.10. Adsorption studies

Mesoporous silicotitaniumphosphate has been used as adsorbent for the removal of toxic metal ions like As(III/V), Cd(II) and Hg(II) from their respective aqueous solutions. In Table 1 chloride exchange capacity for MSTP-Cal sample is given. For metallophosphate materials due to the presence of imbalanced positive charge in the framework could be responsible for the anion exchange capacity as observed for mesoporous titanium- [33], tin- [34] and niobiumphosphate [35] materials. Moderately good ion-exchange capacity of the mesoporous silicotitaniumphosphate material has motivated us to explore its potential in removing pollutant metals

Table 2
Toxic metal uptake by mesoporous silicotitaniumphosphate.^a

Entry	Solution type	Metal content (mg/l)		Metal adsorption efficiency (%)
		Before	After	
1	~200 ppb As(III)	0.208	0.0856	57.2
2	~200 ppb As(III) + 0.05 g H ₂ O ₂	0.208	0.015	92.5
3	~200 ppb Hg(II)	0.203	0.061	69.2
4	~200 ppb Cd(II)	0.205	0.058	71.7
5	~1000 ppb As(III)	0.832	0.359	56.8
6	~1000 ppb Hg(II)	0.941	0.227	75.9
7	~1000 ppb Cd(II)	1.034	0.235	74.3

^a As(III/V), Cd(II) and Hg(II) concentrations before and after the adsorption studies are measure by AAS.

from the waste water. Arsenic is found in its most common valence state as arsenate As(V), in aerobic surface water and as arsenite, As(III), in anaerobic ground water. In the low pH range (4–8) the predominant As(V) species are H₂AsO₄⁻ and HAsO₄²⁻ [36], which are negatively charged and thus easy to get exchanged by an ion

exchanger. In other hand, As(III) remained mostly in nonionised form H₃AsO₃ can easily be oxidized by mild oxidants like H₂O₂. In Table 2 arsenic removal efficiencies of MSTP-Cal from ~200 ppb arsenic containing NaAsO₂ solution with or without addition of small amount of H₂O₂ have been given. As seen from the results

Table 3
Liquid phase benzylation reactions over mesoporous silicotitaniumphosphate.^a

Substrate	Product	Time (h)	Conversion (%)	Selectivity (%)
	 	24	98.9	48.7
		24	43.5	100
		24	29.2	100

^a Reaction conditions: temperature 353 K, substrate: benzyl chloride = 10:1.

that As(V) is more effectively adsorbed over the sample than As(III), which agrees quite well with our previous results on mesoporous silicotinphosphate material [14]. A relatively higher concentration of As(III) (~1000 ppb) similarly show moderate uptake efficiency (Table 2). For the determination of the Hg removal efficiency ~200 and 1000 ppb HgCl₂ solutions has been taken as stock solutions. After stirring these solutions with MSTP-Cal sample for 2 h each, the concentrations of Hg(II) has been analyzed. Under this condition Hg(II) could exist in the solution as a divalent cation [37] and this could be efficiently adsorbed at the defect P–O[−] sites. A considerably high Hg(II) adsorption efficiencies (69.2 and 75.9%) has been observed over our mesoporous silicotitaniumphosphate material. Similarly MSTP-Cal showed good Cd(II) adsorption efficiencies for the respective Cd(II) containing solutions (Table 2). These As(III/V), Cd(II) and Hg(II) adsorption efficiencies are comparable to the mesoporous PMO material LHMS-2 [38] containing electron donor sites in the pore walls. Due to good adsorption efficiencies for As(III/V) and Hg(II), the MSTP-Cal material can be used as adsorbent for the removal of toxic metals from contaminated water.

3.11. Liquid phase catalysis

The liquid phase acid catalyzed Friedel–Crafts benzylation reaction is carried out over this MSTP-Cal material to explore the catalytic performance of it. The result of the reaction is shown in Table 3. As seen from the table, 98.9% *m*-cresol, 43.5% *p*-xylene, 29.2% mesitylene have been benzylated over mesoporous silicotitaniumphosphate over a period of 24 h. For *m*-cresol two benzylated products corresponding to the *para*-adduct of the phenolic-OH and methyl groups (Table 3) are formed in almost equal proportions. On the other hand for *p*-xylene and mesitylene only one respective monobenzylated product is formed exclusively. This result indicates a moderately strong surface acidity of the MSTP-Cal material. To compare the catalytic activity of MSTP-Cal with related mesoporous material, we have chosen a mesoporous aluminosilicate material AISBA-15 [39]. Our synthesized catalyst MSTP-Cal shows much higher activity with respect to this mesoporous material. For *p*-xylene and mesitylene the conversions are 43.5 and 29.2, respectively, over our MSTP-Cal, while it was 23.55 and 17.52%, respectively, over AISBA-15(45). Hence it can be concluded that compared to the other representative solid acid catalysts with mesopores and similar range of surface area our mesoporous MSTP-Cal material has much higher catalytic activity.

Our experimental results suggested that Ti, P, Si atoms are uniformly connected via O centers in our mesoporous silicotitaniumphosphate material. In this mesoporous framework Si and Ti are neutral in nature but one positive charge can reside on P atom, which can be balanced by the counter anions similar to the mesoporous silicotinphosphate material [14]. Thus high anion exchange (due to framework charge) and the metal ion adsorption efficiencies (due to P–O[−] sites) of the material can be explained. Further, presence of defect P–OH/Ti–OH sites (which could result due to H-bonding interaction with F127 molecules at the surface) could be responsible for its strong acid catalytic property.

4. Conclusions

From our experimental observations we can conclude that mesoporous silicotitaniumphosphate material having a good surface area can be synthesized using triblock co-polymer F127 as the SDA and an unconventional phosphorous source trimethylphosphate under evaporation induced self-assembly method. Detailed

characterization results revealed the wormhole-like disordered mesopores in the sample with an average pore dimension of 5.4 nm. The spectroscopic data suggest that most of the Ti sites present in this sample are tetrahedrally co-ordinated Ti(IV). Adsorption of environmentally toxic As(III/V), Cd(II) and Hg(II), and catalytic activity in liquid phase Friedel–Crafts benzylation of aromatics over this novel mesoporous material could open up new opportunities in future.

Acknowledgements

AB wishes to thank Department of Science and Technology, India for financial supports. MP and NP are thankful to the CSIR, New Delhi for their senior research fellowships.

References

- [1] C.T. Kresge, M.E. Leonowicz, W.J. Roth, J.C. Vartuli, J.S. Beck, *Nature* 359 (1992) 710–712.
- [2] S. Inagaki, Y. Fukushima, K. Kuroda, *J. Chem. Soc. Chem. Commun.* (1993) 680–682.
- [3] D.P. Das, K.M. Parida, *J. Mol. Catal. A: Chem.* 276 (2007) 17–23.
- [4] T.M. Suzuki, T. Nakamura, K. Fukumoto, M. Yamamoto, Y. Akimoto, K. Yano, *J. Mol. Catal. A: Chem.* 280 (2008) 224–232.
- [5] Y. Kubota, C. Jin, T. Tatsumi, *Catal. Today* 132 (2008) 75–80.
- [6] S. Benmokhtar, H. Belmal, A.E. Jazouli, J.P. Chaminade, P. Gravereau, S. Pechev, J.C. Grenier, G. Villeneuve, D. de Waal, *J. Solid State Chem.* 180 (2007) 772–779.
- [7] C. Pan, S. Yuan, W. Zhang, *Appl. Catal. A: Gen.* 312 (2006) 186–193.
- [8] M. Paul, N. Pal, B.S. Rana, A.K. Sinha, A. Bhaumik, *Catal. Commun.* 10 (2009) 2041–2045.
- [9] A. Bhaumik, S. Inagaki, *J. Am. Chem. Soc.* 123 (2001) 691–696.
- [10] D. Jing, L. Guo, *J. Phys. Chem. C* 111 (2007) 13437–13441.
- [11] A. García, M. Colilla, I.I. Barba, M.V. Regi, *Chem. Mater.* 21 (2009) 4135–4145.
- [12] N. Ikawa, Y. Oumi, T. Kimura, T. Ikeda, T. Sano, *J. Mater. Sci.* 43 (2008) 4198–4207.
- [13] B. Boddenberg, V. Radha Rani, R. Grosse, *Langmuir* 20 (2004) 10962–10969.
- [14] D. Chandra, N.K. Mal, A. Bhaumik, *J. Mol. Catal. A: Chem.* 247 (2006) 216–221.
- [15] D. Zhao, J. Feng, Q. Huo, N. Melosh, G.H. Fredrickson, B.F. Chmelka, G.D. Stucky, *Science* 279 (1998) 548–552.
- [16] W. Chen, Y. Geng, X.-D. Sun, Q. Cai, H.-D. Li, D. Weng, *Micropor. Mesopor. Mater.* 111 (2008) 219–227.
- [17] H. Peng, J. Tang, L. Yang, J. Pang, H.S. Ashbaugh, C.J. Brinker, Z. Yang, Y. Lu, *J. Am. Chem. Soc.* 128 (2006) 5304–5305.
- [18] K. Nakajima, I. Tomita, M. Hara, S. Hayashi, K. Domen, J.N. Kondo, *Adv. Mater.* 17 (2005) 1839–1842.
- [19] S. Benmokhtar, A. El jazouli, J.P. Chaminade, P. Gravereau, M. Menetrier, F. Bouree, *J. Solid State Chem.* 180 (2007) 2713–2722.
- [20] K. Sarkar, M. Nandi, A. Bhaumik, *Appl. Catal. A: Gen.* 343 (2008) 55–61.
- [21] K. Sarkar, T. Yokoi, T. Tatsumi, A. Bhaumik, *Micropor. Mesopor. Mater.* 110 (2008) 405–412.
- [22] D.Q. Yang, M. Meunier, E. Sacher, *J. Appl. Phys.* 98 (2005) 114310–114316.
- [23] W. Zhang, M. Fröba, J. Wang, P.T. Tanev, J. Wong, T.J. Pinnavaia, *J. Am. Chem. Soc.* 118 (1996) 9164–9171.
- [24] M. Anpo, H. Yamashita, Y. Ichihashi, Y. Fujii, M. Honda, *J. Phys. Chem. B* 101 (1997) 2632–2636.
- [25] Y.X. Li, C.F. Xie, S. Peng, G.W. Lu, S.B. Li, *J. Mol. Catal. A: Chem.* 282 (2008) 117–123.
- [26] D.T. On, L. Bonnevoit, A. Bittar, A. Sayari, S. Kaliaguine, *J. Mol. Catal.* 74 (1992) 233–246.
- [27] Y.S.S. Wan, J.L.H. Chau, K.L. Yeung, A. Gavriilidis, *J. Catal.* 223 (2004) 241–249.
- [28] S. Baunack, S. Oswald, D. Scharnweber, *Surf. Interface Anal.* 26 (1998) 471–479.
- [29] T.Z. Ren, Z.Y. Yuan, A. Azioune, J.J. Pireaux, B.L. Su, *Langmuir* 22 (2006) 3886–3894.
- [30] D. Akolekar, A. Chaffee, R.F. Howe, *Zeolite* 19 (1997) 359–365.
- [31] K. Chaudhari, T.K. Das, P.R. Rajamohanam, K. Lazar, S. Sivasanker, A.J. Chandwadkar, *J. Catal.* 183 (1999) 281–291.
- [32] J.D. Epping, B.F. Chmelka, *Curr. Opin. Colloid Interface Sci.* 11 (2006) 81–117.
- [33] R. Ryoo, S.H. Joo, M. Kruk, M. Jaroniec, *Adv. Mater.* 13 (2001) 677–681.
- [34] N.K. Mal, S. Chikawa, M. Fujiwara, *Chem. Commun.* 2 (2002) 112–113.
- [35] N.K. Mal, A. Bhaumik, P. Kumar, M. Fujiwara, *Chem. Commun.* 7 (2003) 872–873.
- [36] B. Dousova, V. Machovic, D. Kolousek, F. Kovanda, V. Dornicak, *Water Air Soil Pollut.* 149 (2003) 251–267.
- [37] P. Miretzky, A.F. Cirelli, *J. Hazard. Mater.* 167 (2009) 10–23.
- [38] D. Chandra, S.K. Das, A. Bhaumik, *Micropor. Mesopor. Mater.* 128 (2010) 34–40.
- [39] A. Vinu, D.P. Sawant, K. Ariga, M. Hartmann, S.B. Halligudi, *Micropor. Mesopor. Mater.* 80 (2005) 195–203.